Method used to measure interaction of proteins with dual-beam optical tweezers

E. Qu
Honglian Guo
Chunhua Xu
Chinese Academy of Sciences
Institute of Physics
Beijing National Laboratory for Condensed Matter Physics
P. O. Box 603
Beijing 100080, China
E-mail: que@aphy.iphy.ac.cn

Chunxiang Liu
Shandong Normal University
Department of Physics
Jinan, Shandong 250014, China

Zhaolin Li
Bingying Cheng
Daozhong Zhang
Chinese Academy of Sciences
Institute of Physics
Beijing National Laboratory for Condensed Matter Physics
P. O. Box 603
Beijing 100080, China

Abstract. In the force measurement of protein-protein interaction, proteins are usually attached to microbeads, so the coated beads serve as both handles and force transducers. Due to the short interaction distance between proteins, the beads are usually close enough to each other. When dual-beam optical tweezers and quadrant photodiode detector are used to investigate the interaction of proteins, it is found that the signal of detected beads is greatly affected by adjacent beads. Analysis reveals that the contribution of two beads to the quadrant detector signal is independent. A method for extracting the real interaction signal from a disturbed one is presented. Based on this method, interaction between microtubules and AtMAP65-1 is measured. The results show that this method is useful for measuring short-distance interaction with the precision of piconewton and nanometer scales.
 [DOI: 10.1117/1.2397575]

Keywords: optical tweezers; quadrant photodiode detector; protein interaction.

Paper 06023RR received Feb. 7, 2006; revised manuscript received Aug. 7, 2006; accepted for publication Aug. 7, 2006; published online Nov. 20, 2006.

1 Introduction

Recently, the study of properties, functions, and interactions of proteins has fascinated people. It has become one of the most important fields in life sciences. People analyze labeled genes to build databases for meaningful interactions of protein systems. Therefore, studies of the interaction of proteins have attracted significant attention. Correspondingly, different techniques have been used to perform these kinds of experiments, such as atomic force microscopy (AFM),[1–4] hydrodynamic methods,[5,6] biomembrance force probes (BFP) with pipette suction,[7,8] and optical tweezers.[9–17] Among these tools, optical tweezers have emerged as a widely used and versatile tool to investigate interactions of protein-protein, protein-DNA, and protein-RNA. Mechanics of motor molecules (kinesin,[9] myosin[10]), interactions of matrix-integrin-cytoskeletons,[11] fibroblasts- fibronectin,[12] IgG-protein A,[13] RNAP-DNA,[14,15] Fibrinogen-Integrin αIIbβ3,[16] Helicobacter pylori adhesin BabA-Lewis b blood group antigein,[17] and other proteins have been studied with optical tweezers. In some experiments, proteins of interest are attached to the trapped bead, then contact their targets (proteins, DNA, microtubules, and so on) that are fixed on the coverglass surface. By measuring displacement of the trapped bead, one can get interacting properties between the protein and targets. However, such measurements may introduce mechanical instability and strong instrumental shift due to the instability of the coverglass surface, which means that precision will be greatly limited.[18] Using dual-beam optical traps, however, can avoid the mechanical instability to some extent because none of the components of the assay are attached to the coverglass. This isolates the system from drift of the microscope stage and significantly improves the precision of measurements. In the measurement of protein interaction with dual-optical tweezers, proteins are attached to the surface of the "handles"—trapped beads. A quadrant photodiode detector (QD) is widely used to detect the movement of the concerned bead.[16,19–21] When measuring an interaction of protein-protein, two beads should be close to each other (in the magnitude of 10 nm) because the interaction distance of proteins is short. However, when the distance between the two beads is small, the image of undetected bead will come into the detecting area of the QD inevitably. Consequently, it is difficult to get correct information directly because the output signal is seriously disturbed. To reduce the disturbance, flexible tethers are adopted to act as linkers between proteins and bead in some experiments.[22,23] In doing so, the direct contact of two beads is avoided. Therefore, the influence of one bead to the other is eliminated when measuring a protein-protein interaction with the QD. However, the introduction of tether makes the data analysis more complicated, owing to the contribution of the tether to the measured interaction force and distance. To make the concerned system as simple as possible,

Address all correspondence to E. Qu, Optical Physics Lab, Beijing National Lab for Condensed Matter Physics, Institute of Physics, Chinese Academy of Sciences, P. O. Box 603-29, Beijing, Beijing 100080 China; Tel.: 86-10-82649340; Fax: 86-10-82649451; E-mail: que@aphy.iphy.ac.cn

1083-3668/2006/11(6)/064035/6/$22.00 © 2006 SPIE

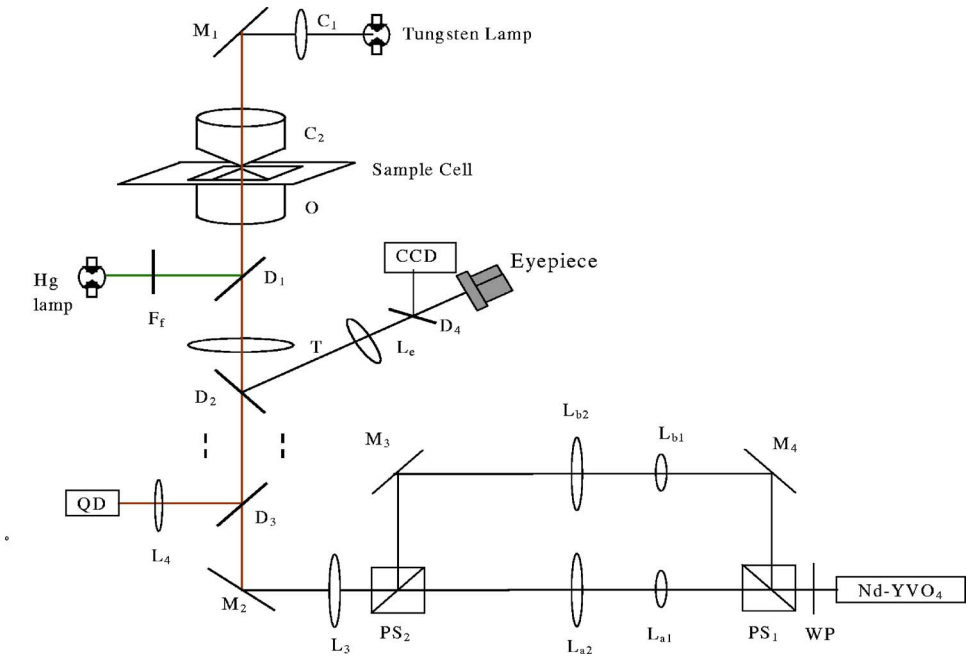

Fig. 1 Schematic diagram of the dual-beam optical tweezer system. WP, half-wave plate; PS_1 and PS_2, polarizing beamsplitter cubes; L_{a1}, L_{a2}, L_{b1}, and L_{b2}, lenses for beam expanding; M_1, M_2, M_3, and M_4, mirrors for beam steering; O, microscopy objective; C_1 and C_2, lenses for illumination light condensing; D_1, D_2, D_3, and D_4, dicroic filters; L_4 and L_e, auxiliary lenses for imaging; and F_f, filter lens. lenses L_3 and T (tube lens) are confocal.

people usually tag proteins directly on beads. Different kinds of proteins are tagged on different beads. Additionally, another position sensitive detector, optical trapping interferometry[17,23,24] instead of a QD can reduce this disturbance to some extent. It is very expensive and complex compared with the QD. Therefore, it is of importance to make good use of the QD, since it is still widely used as a fairly simple and precise instrument. In this work, we give an analysis of the disturbance and find that the contribution of two beads together with the QD signal equals the summation of that of each bead alone. Furthermore, we provide a corresponding solution to extract real interaction signals, and measure the interaction between microtubules and AtMAP65-1 (one of the microtubule associated proteins) as an application.

2 Dual Beam Optical Tweezers Setup and Calibration

The schematic diagram of the system is shown in Fig. 1. A 1064-nm beam of a Nd-YVO_4 laser (Coherent, Incorporated, compass 1064 nm) is split into two beams by polarizing beamsplitter cube PS_1. Then, two expanded beams are coupled into an inverted microscope (Leica, DMIRB) with a high numerical aperture objective (Leica, HCX PL APO, 100×, NA=1.4) to form dual-optical tweezers. One trap can move in the horizontal plane by rotating the reflected mirror M_3 driven by a dc servomotor (Newport, LTA-HL Actuator), while the other is fixed. Uniform polystyrene beads with diameters of 1 μm are used as handles. The bead trapped in the fixed trap, which is defined as a detected bead, is illuminated by a 100-W tungsten lamp. After being magnified 100 times and 5 times by objective and the auxiliary lens L_4, respectively, its image is projected onto the front surface of the QD, which is initially set homocentric with the image of the bead in the center of the fixed trap, so that the deviation of the bead in the fixed trap can be detected by the QD. A high-resolution cooled charge-coupled device (CCD) (Coolsnap fx, USA) is used to record the series of two bead images.

Displacement of a bead from the trap center, and consequently the force exerted by the trap on the displaced bead, can be measured with the quadrant detector. The output currents from the four quadrants of the photodiodes are converted to voltages, then the four voltages are combined to yield two voltages that are proportional to the displacements in the x and y directions. Both signals are sampled at 1 kHz, and recorded on a PC via an analog-to-digital converter board. The relationship between the QD voltage and bead displacement can be determined, according to Refs. 20 and 21. The corresponding transfer coefficient of the voltage to the bead displacement in the x direction is 2.5 ± 0.1 mV/nm. Force calibration and trap stiffness are routinely confirmed by the Stokes' force method.[20,21] In our experiments, the stiffness of both traps is 0.20 ± 0.01 pN/nm at a laser power of 260 mW for each beam measured in the front of the objective back aperture. The velocity of a movable trap in our experiments is $v=74\pm1$ nm/s.

3 Disturbance in Quadrant Detector Detection

When two independent beads come close to each other, the image of the moving bead (undetected bead) will come into the detecting area of the QD. As a result, measurement of the displacement of the detected bead will be disturbed. A micrograph of two trapped beads that are magnified 500 times and projected onto the front surface of a QD is shown in Fig. 2. Distance between the centers of two beads is 1.3 μm. A

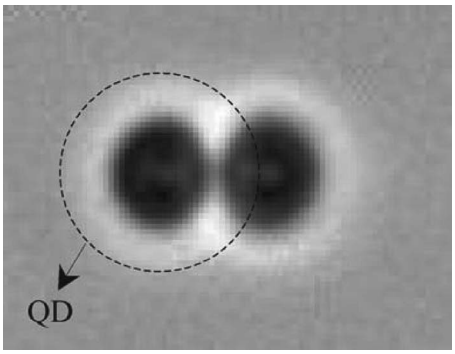

Fig. 2 Image of two trapped beads magnified 500 times and projected onto the front surface of a QD (dashed circle). The distance between the centers of two beads is 1.3 μm (corresponding to 0.65 mm after being magnified 500 times).

dashed circle represents the front surface of a QD whose diameter is 1 mm. It is obvious that a part of the undetected bead image (right bead) is in the detecting area of the QD. Consequently, the output signal of a QD varies when an undetected bead is moved away while the detected bead remains immobile, which means that the signal of the QD has been disturbed by the moving bead, and it does not represent real deviation of the detected beads from the trap center anymore.

To receive a real interaction signal from a disturbed one, we must make two issues clear. The first is whether the disturbed output signal is repeatable or not. Second, we should know the origin of the disturbance, especially if there is interference between the images of the two beads.

A series of experiments is carried out to check the repeatability of background signals. The output background signal of a QD is recorded when the undetected bead is moved away from the position where the two beads are in contact. Such experiments are repeated several times to receive the disturbance background signal curves. The starting position of the undetected bead is guaranteed to be the same for each experiment by the dc servomotor. Two results are shown in Fig. 3(a) (marked by solid and dotted lines), in which two curves coincide well. Then an average background signal is obtained over 11 measurements, as shown in Fig. 3(b), where the high frequency signals caused by the Brownian noise are filtered. Bars in the curve indicate a standard deviation of the y coordinate over 11 measurements. It is clearly seen that the disturbance background voltage has good repeatability.

In addition, when external force is applied to the bead, the detected bead will deviate instead of staying at the center of the QD. To know whether the background signal is repeatable under different conditions where the detected bead is in or off the center of the QD, more experiments are carried out. First, the QD is adjusted 50 nm away from the center of the detected bead. Then another bead is caught in the moving trap and the measurements are done following the previous procedure. One of the experimental results is shown in Fig. 3 (marked by a dashed line), and it is about 125 mV lower than the detected bead in the trap center. −125 mV exactly corresponds to 50-nm displacement of a detected bead, since the transfer coefficient between the voltage and the displacement of the detected bead is 2.5 mV/nm. Furthermore, similar experiments are carried out when the QD is moved 100 and 150 nm away from the center of the detected bead (experiment curves are not shown here). All the results indicate that the background signal is repeatable.

To know whether interference exists or not between two bead images, we carry out two experiments (Fig. 4). At first, following the prior experimental procedure, the output signal of the QD is recorded when both the detected and undetected beads are present. Then, the measurement is repeated under the condition that only the undetected bead remains, and the starting position of the moving bead is also set the same as the previous experiments by motor. It is clearly seen that the two signals coincide well. Therefore, it can be concluded that the disturbance is completely from the moving bead.

When the image of the moving bead comes into the detecting area of a QD, the two beads are very close to each other.

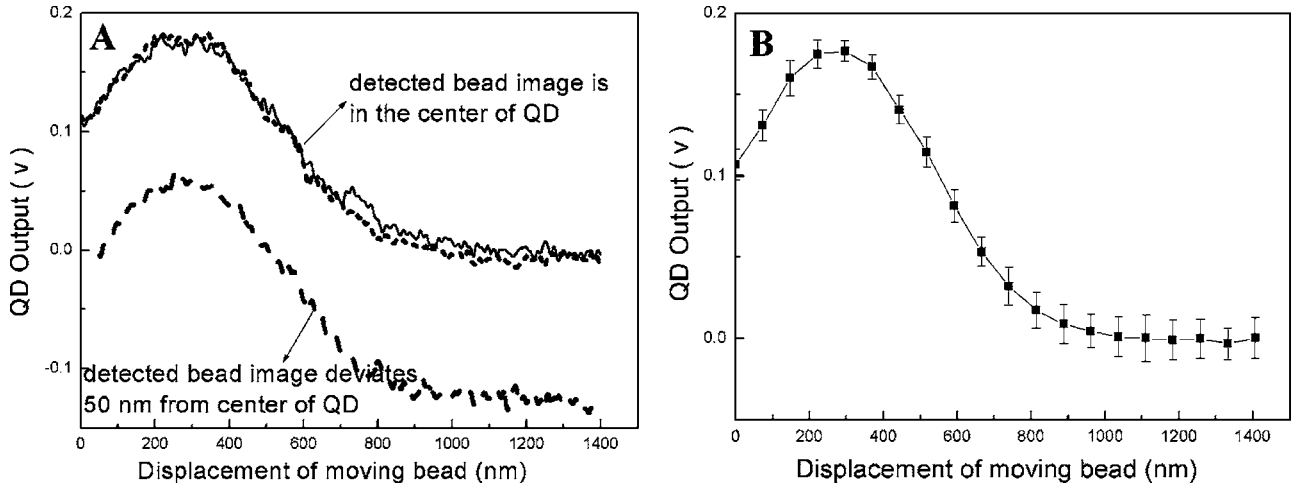

Fig. 3 (a) Output signals versus displacement of moving bead. The zero point in the x axis corresponds to the starting position of the moving bead when the detected bead is in the center of the QD. When the detected bead is 50 nm out of the center of the QD, the starting position is also 50 nm away from the zero point. (b) The average background signal of 11 experiments measured when the detected bead image is in the center of the QD. Bars indicate the standard deviation of the y coordinate over 11 measurements.

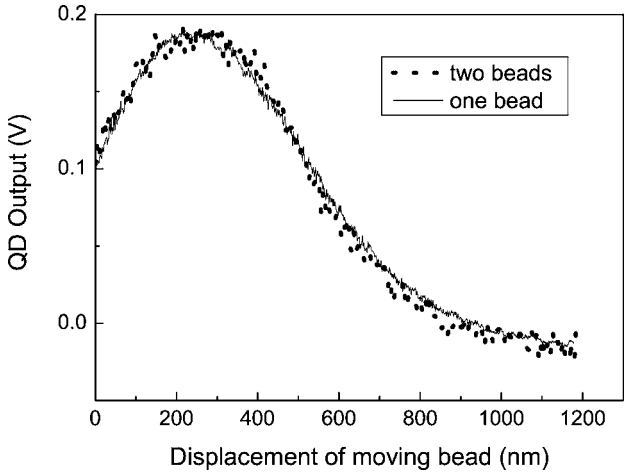

Fig. 4 Dependence of the output signal on the displacement of the moving bead. The solid and dotted lines are the experimental results under the conditions that only the moving bead exists and both detected and moving beads exist, respectively.

Generally speaking, the interference may occur when a light beam passes through two closed beads. However, there is little influence on the output signals as measured before. It is probably due to the illuminating source (tungsten lamp) and illuminating mode (Kohler illumination) we chose. These make the effect of interference negligible. It implies that the contributions of the two bead images to the QD are independent. In addition, the disturbance signal is not monotonic but parabolic with the displacement of the undetected bead. This is due to the fact that the intensity of the bead image is not homogeneous, as shown in Fig. 2. There is a much brighter ring in the fringe of the bead image. The contributions of both the dark field and bright ring of the bead image result in this parabolic disturbance curve.

4 Method for Extracting Real Interaction Signals

When the interaction between two beads exists, usually we displace the movable trap at a certain velocity and detect the displacement of the bead in the fixed trap to know the interaction distance and force. The displacement of the detected bead can be extracted by deducting the disturbance background of the moving bead from the total output signal. However, in this case, not only does the detected bead move, but also the bead in the movable trap deviates from its trap center. This is quite different from no interaction between beads. When there is interaction, the undetected bead deviates from the center of the movable trap. Consequently, the displacement of the moving bead no longer equals the product of time and velocity of the movable trap, which means that the displacement of the moving bead when there is interaction is not synchronous with no interaction between two beads. Therefore, a disturbance cannot be deducted directly from the total output signal. To deduct the disturbance background signal, we should shift the time coordinate of the background signal to find the point where the displacement of the moving bead is the same as that with interaction. Time t is shifted to

$$t' = t - \frac{CX_a(t)}{v},$$

where v is the velocity of the movable trap, $X_a(t)$ is the displacement of the detected bead, and $CX_a(t)$ is the corresponding displacement of the undetected bead from the movable trap (C is the stiffness ratio of the fixed trap to the movable one). We should deduct the disturbance signal at time t' rather than t. The relationship of background signal $V_{back}(t')$, total output signal $V_{total}(t)$, and real interaction signal $K_{\mathrm{QD}}X_a(t)$ can be expressed by the following equation:

$$V_{\mathrm{total}}(t) = V_{\mathrm{back}}(t') - K_{\mathrm{QD}} \times X_a(t), \tag{1}$$

where K_{QD} is the transfer coefficient between the voltage and the displacement of the detected bead of the QD, which is 2.5 ± 0.1 mV/nm. $V_{total}(t)$ and $V_{back}(t)$ are measured in the experiments, then the displacements $X_a(t)$ can be obtained by numerical fitting, and consequently the corresponding interaction force can be found.

To estimate the measurement precision in our experiments $\Delta X_a(t)$, the standard deviation of $X_a(t)$ can be obtained from standard deviations of K_{QD}, $V_{total}(t)$ and $V_{back}(t')$ according to Eq. (1). However, it is complicated due to the fact that $X_a(t)$ also exists in the term $V_{back}(t')$. Therefore, an iterative calculation is carried out by the following expression until the final result converges:

$$\left(\frac{\Delta_i X_a}{X_a}\right)^2 = \left(\frac{\Delta V_{\mathrm{total}}(t)}{K_{qd} \times X_a}\right)^2 + \left(\frac{\Delta V_{\mathrm{back}}(t)}{K_{qd} \times X_a}\right)^2 + \left(\frac{\dfrac{\partial V_{\mathrm{back}}(vt)}{\partial (vt)} \times C \times \Delta_{i-1} X_a}{K_{qd} \times X_a}\right)^2 + \left(\frac{\Delta K_{qd}}{K_{qd}}\right)^2 \quad i = 1,2,3,\ldots \tag{2}$$

$\Delta_0 X_a(t)$ is set to be zero. Based on Fig. 3, both $\Delta V_{total}(t)$ and $\Delta V_{back}(t)$ are taken to be 9.9 mV, and $\partial V_{back}(vt)/\partial(vt)$ is taken as its maximum value 0.4 mV/nm. Through calculation, $\Delta X_a(t)/X_a(t)$ is 6.97% when $X_a(t)$ is 100 nm (corresponding force is 20 pN), and 4.95% when $X_a(t)$ is 200 nm (corresponding force is 40 pN). Subsequently, the corresponding error of force is 1.39 and 1.98 pN, respectively.

5 Application

It has been reported that AtMAP65-1 induces the formation of large microtubule bundles by forming cross-bridges between microtubules.[25] The bundling of microtubules in interphase in plant cells has been suggested to be important for the formation of the interphase cortical array.[26] Moreover, in the presence of AtMAP65-1, microtubule bundles were more resistant to cold and dilution treatments.[25] Therefore, the interaction between microtubules and AtMAP65-1 is crucial, since it can directly affect the mechanical properties of microtubules, and further the organizations and some functions of microtubules. To quantitatively know the interaction between a microtubule (MT) and microtubule associated protein (AtMAP65-1), we measure the unbinding force between them. The microstructure of microtubule bundles cross-linked by AtMAP65-1 is shown in Fig. 5(a).[25]

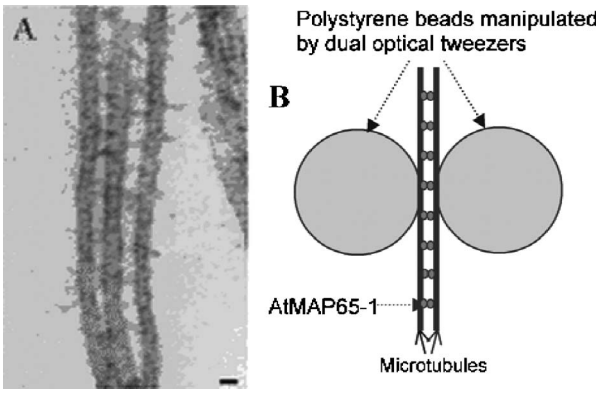

Fig. 5 (a) Electron micrograph of microtubule bundles cross-linked by AtMAP65-1.[25] (b) Schematic illustration of the measurement of interaction between a microtubule and AtMAP65-1.

After being assembled *in vitro* following established recipes,[27] a microtubule (MT) is centrifuged and stabilized by 0.1-mol/L Pipes, 1 mmol/L EGTA, 1-mmol/L MgSO4, 10-μM taxol, and 10%DMSO, pH 6.9 (PEMT). Then the MT is suspended in solution. Large microtubule bundles were formed after adding AtMAP65-1 to the solution, and the molar ratio of tubulin to AtMAP65-1 is 7:1.

We manipulate two trapped beads to make the two beads attached to the microtubule bundle. Due to the specific adhesion of biotin-neutravidin, a stable combination between the bundle and beads is formed. Schematic illustration of this bead-MT-AtMAP65-1-MT-bead sandwich-like formation is exhibited in Fig. 5(b). To get a symmetrical load on a microtubule bundle, we make sure that the bundle chosen for adhesion is perpendicular to the moving direction of a movable trap. As long as the combination is achieved, the trap moves with a velocity of 74 nm/s; meanwhile, the time course of the output signal is recorded [Fig. 6(a), marked with a solid line]. When the rigor bonds between microtubule and AtMAP65-1 are broken, the beads return to the trap centers. The diameter of the bundle (near several hundred nanometers) is so small compared with the beads that two beads should be very close to each other. Therefore, the influence of a moving bead cannot be neglected. We do another control experiment when there is no interaction between the two beads to get a background signal. After the beads return to the trap centers, we move the right bead again close to the left bead. Adhesion should not occur during this procedure. After the two beads are close to each other, the right trap is moved far from the fixed trap with a velocity of 74 nm/s. The output signal of the QD is considered the background signal [Fig. 6(a), marked with a dotted line]. With the method introduced earlier, real interaction signal is extracted [Fig. 6(b)] and the measured unbinding force is 14.7 pN. Furthermore, the interaction distance is determined to be 3 nm from the force curve [interaction distance is the displacement of the trap and deviations of the beads from trap centers. Detailed calculation is given as follows: $2.030\ \text{s} \times 74\ \text{nm/s} - 2 \times 73.5\ \text{nm} \approx 3\ \text{nm}$, where 2.030 s, which is the time span from the starting position to the point where unbinding occurs, is obtained from Fig. 6(b). 73.5 nm is the deviation from the trap centers of each bead—$73.5\ \text{nm} \times 0.20\ \text{pN/nm} = 14.7\ \text{pN}$. Because both beads deviate from the trap centers, total deviations are 2×73.5 nm]. Therefore, the unbinding energy is 5.4 K_BT (22 pN·nm) ($1/2\ F_{\text{unbinding}}$ interaction distance). More studies are in progress, and we expect that this method can be used to obtain more precise information about the interaction between proteins.

6 Conclusion

The interaction force of proteins can be measured with dual-optical tweezers and a photodiode quadrant detector (QD). It is found that the output signal of the QD is significantly affected by the undetected bead due to the short distance between the two beads. We demonstrate experimentally that contributions of two bead images to the QD are independent. The disturbed signal completely comes from the image of the undetected bead in a movable trap. Therefore, the total output signal measured when there is interaction is the sum of a real interaction signal and the disturbed one. Subsequently, a method used for extracting the real interaction signal is obtained. As an application, the interaction force between microtubules and AtMAP65-1 is measured. It is clearly seen that short-distance interaction can be measured with high precision by using dual-optical tweezers. This meets the needs for

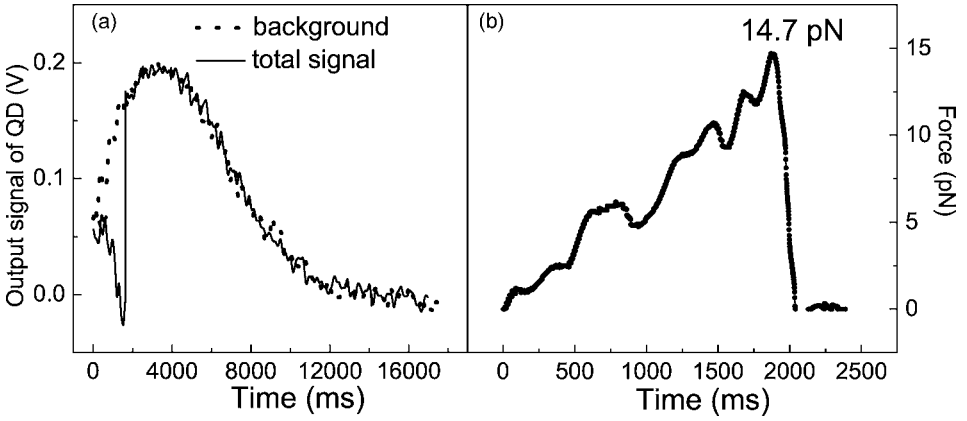

Fig. 6 (a) Background signal (there is no interaction) and total output signal (there is interaction). (b) Result of interaction force between microtubule and AtMAP65-1.

studying the interaction properties of proteins.

Acknowledgments

This work was supported by the Chinese National Key Basic Research Special Fund (grant number 2002CB713805) and the National Natural Science Foundation of China (grant number 10374112).

References

1. A. L. Chen and V. T. Moy, "Single-molecule force measurements," in *Atomic Force Microscopy in Cell Biology*, B. P. Jena and J. K. H. Horber, Eds., pp. 301–309, Academic Press, San Diego, CA (2002).
2. E. L. Florin, V. T. Moy, and H. E. Gaub, "Adhesion forces between individual ligand-receptor pairs," *Science* **264**, 415–417 (1994).
3. G. U. Lee, L. A. Chris, and R. J. Colton, "Direct measurement of the forces between complementary strands of DNA," *Science* **266**, 771–773 (1994).
4. V. T. Moy, E. L. Florin, E. L. Florin, and H. E. Gaub, "Intermolecular forces and energies between ligands and receptors," *Science* **266**, 257–259 (1994).
5. D. F. J. Tees and H. L. Goldsmith, "Kinetics and locus of failure of receptor-ligand-mediated adhesion between latex spheres. I. Protein-carbohydrate bond," *Biophys. J.* **71**, 1102–1114 (1996).
6. D. Kwong, D. F. J. Tees, and H. L. Goldsmith, "Kinetics and locus of failure of receptor-ligand-mediated adhesion between latex spheres. II. Protein-protein bond," *Biophys. J.* **71**, 1115–1122 (1996).
7. J. Y. Shao and R. M. Hochmuth, "Mechanical anchoring strength of L-selectin,_integrins, and CD45 to neutrophil cytoskeleton and membrane," *Biophys. J.* **77**, 587–596 (1999).
8. J. Y. Shao and R. M. Hochmuth, "Micropipette suction for measuring piconewton forces of adhesion and tether formation from neutrophil membranes," *Biophys. J.* **71**, 2892–2901 (1996).
9. K. Svoboda, C. F. Schmidt, S. B. J. Chnapp, and S. M. Block, "Direct observation of kinesin stepping by optical trapping interferometry," *Nature (London)* **365**, 721–727 (1993).
10. T. Nishizaka, H. Miyata, H. Yoshikawa, S. Ishiwate, and K. K. Jr., "Unbinding force of a single motor molecule of muscle measured using optical tweezers," *Nature (London)* **377**, 251–254 (1995).
11. G. Jiang, G. Giannone, D. R. Critchley, E. Fukumoto, and M. P. Sheetz, "Two-piconewton slip bond between fibronectin and the cytoskeleton depends on talin," *Nature (London)* **424**, 334–337 (2003).
12. O. Thoumine, P. Kocian, A. Kottelat, and J. J. Meister, "Short-term binding of fibroblasts to fibronectin: optical tweezers experiments and probabilistic analysis," *Eur. Biophys. J.* **29**, 398–408 (2000).
13. A. L. Stout, "Detection and characterization of individual intermolecular bonds using optical tweezers," *Biophys. J.* **80**, 2976–2986 (2001).
14. M. D. Wang, M. J. Schnitzer, H. Yin, R. Landick, J. Gelles, and S. M. Block, "Force and velocity measured for single molecules of RNA polymerase," *Science* **282**, 902–907 (1998).
15. H. Yin, M. D. Wang, K. Svoboda, R. Landick, S. M. Block, and J. Gelles, "Transcription against an applied force," *Science* **270**, 1653–1657 (1995).
16. R. I. Litvinov, J. S. Bennett, J. W. Weisel, and H. Shuman, "Multi-step fibrinogen binding to the integrin αIIbβ3 detected using force spectroscopy," *Biophys. J.* **89**, 2824–2834 (2005).
17. O. Björnham, E. Fällman, O. Axner, J. Ohlsson, U. J. Nilsson, T. Borén, and S. Schedin, "Measurements of the binding force between the *Helicobacter pylori* adhesin BabA and the Lewis b blood group antigen using optical tweezers," *J. Biomed. Opt.* **10**, 044024 (2005).
18. A. D. Mehta, M. Rief, J. A. Spudich, D. A. Smith, and R. M. Simmons, "Single-molecule biomechanics with optical methods," *Science* **283**, 1689–1695 (1999).
19. H. L. Guo, C. H. Xu, C. X. Liu, E. Qu, M. Yuan, Z. L. Li, B. Y. Cheng, and D. Z. Zhang, "Mechanism and dynamics of breakage of fluorescent microtubules," *Biophys. J.* **90**, 2093–2098 (2006).
20. H. L. Guo, C. X. Liu, Z. L. Li, J. F. Duan, X. H. Han, B. Y. Cheng, and D. Z. Zhang, "Displacement and force measurements with quadrant photodetector in optical tweezers," *Chin. Phys. Lett.* **20**, 950–952 (2003).
21. R. M. Simmons, J. T. Finer, S. Chu, and J. A. Spudich, "Quantitative measurements of force and displacement using an optical trap," *Biophys. J.* **70**, 1813–1822 (1996).
22. C. Jeppesen, J. Y. Wong, T. L. Kuhl, J. N. Israelachvili, N. Mullah, S. Zalipsky, and C. M. Marques, "Impact of polymer tether length on multiple ligand-receptor bond formation," *Science* **293**, 465–468 (2001).
23. S. Kulin, R. Kishore, J. B. Hubbard, and K. Helmerson, "Real-time measurement of spontaneous antigen-antibody dissociation," *Biophys. J.* **83**, 1965–1973 (2002).
24. A. D. Mehta, M. Rief, J. A. Spudich, D. A. Smith, and R. M. Simmons, "Single-molecule biomechanics with optical methods," *Science* **283**, 1689–1695 (1999).
25. T. L. Mao, L. F. Jin, H. Li, B. Liu, and M. Yuan, "Two microtubule-associated proteins of the arabidopsis MAP65 family function differently on microtubules," *Plant Physiol.* **138**, 1–9 (2005).
26. S. Shaw, R. Kamyar, and D. Ehrhardt, "Sustained microtubules treadmilling in Arabidopsis cortical arrays," *Science* **300**, 1715–1718 (2003).
27. R. C. Williams Jr., and J. C. Lee, "Preparation of tubulin from brain," *Methods Enzymol.* **85**, 376–385 (1982).